JOURNAL OF OPTOELECTRONICS AND ADVANCED MATERIALS Vol. 9, No. 11, November 2007, p. 3489 - 3492

$(Te/SnSe_2)_3$ multilayers deposited by pulsed laser deposition. Structure and gas sensing properties

A. LORINCZI*, F. SAVA, A. TOMESCU, C. SIMION, G. SOCOL[a], I. N. MIHAILESCU[a], M. POPESCU
National Institute R&D of Materials Physics, 077125-Bucharest-Magurele, P. O. Box. MG. 7, Romania
[a]National Institute R&D of Lasers, Plasma and Radiation Physics, 077125-Bucharest-Magurele, P. O. Box MG. 6, Romania

Multilayers made of alternative layers of composition $SnSe_2$ and tellurium (three pairs) have been prepared by pulsed laser deposition (PLD). The complex films have been investigated by X-ray diffraction. After a special annealing in oxygen fluence at various temperatures, up to 620 °C, the films were investigated both by X-ray diffraction and for gas sensing. Gas sensing properties were tested for water vapours, carbon monoxide (CO) and methane (CH_4). After annealing at high temperature, the structure of the multilayer samples show oxide phases like TeO_2, SnO_2 and a mixed oxide ternary phase $SnTe_3O_8$. The annealed multilayers show good sensing properties to water vapours and CO gas.

(Received August 1, 2007; accepted November 1, 2007)

Keywords: Multilayers, Chalcogenides, X-ray diffraction, Gas sensing properties

1. Introduction

The semiconducting oxide gas sensors are the most investigated group of gas sensors. They attracted the attention due to low cost and flexibility in production, as well as large number of possible gases to be detected [1-5]. The detection and identification of pollutant gases is an important task for environmental control. One way to detect the contaminant gases is to use sensitive films that react with the gases and modify the physical parameters, in particular the electrical resistivity.

Various SnO_2 films have been prepared including fluorine-doped films [6]. Cerium-doped SnO_2 has good sensitivity, high selectivity and quick response to CH_4 and H_2S even at room temperature [7, 8]. Films of ZnO to be used as transparent electrodes and sensors have been deposited by spray pyrolysis [9]. Ga_2O_3 has been used as high temperature gas sensor [10]. WO_3 and Pt doped WO_3 nanograin thin films were used as gas sensors [11].

Last years much attention was paid to glassy chalcogenide materials and polymers, as possible materials for gas (electronic nose) and liquid (electronic tongue) sensors [12-22]. On the other hand the pulsed laser method has been developed and applied as an efficient method for thin film deposition [23-29]. Chalcogenide-based thin film sensors have been prepared by pulsed laser deposition [30]. One advantage of the pulsed laser deposition (PLD) method is the stoichiometric transfer of multi-component target material to a given substrate. This advantage of the PLD determined the choice to prepare chalcogenide-based thin films with an off-axis geometry PLD. Ag-As-S and Cu-Ag-As-Se-Te targets were used to deposit thin films on Si substrates for an application as a heavy metal sensing device. The films were characterized by means of Rutherford backscattering spectrometry (RBS), transmission electron microscopy (TEM), and electrochemical measurements. The same stoichiometry of the films and the targets was confirmed by RBS measurements. A good long-term stability of more than 60 days and a nearly Nernstian sensitivity towards Pb and Cu, which is comparable to bulk sensors has been observed.

Recently, we have shown that $SnSe_2$ is a good material for gas sensors, for which a patent request has also been submitted [31].

In this paper we present the results regarding the gas sensing, obtained in the study of a multilayer film made-up by three double layers of $Te/SnSe_2$ prepared by pulsed laser deposition.

2. Experimental

The experiment consisted in the deposition of a multilayer chalcogenide film by pulsed laser deposition, onto Al_2O_3 substrate provided with interdigitated electrodes and platinum heater on the back side.

Firstly a Te film was deposited in the following conditions: KrF* excimer laser, λ = 248 nm, pulse duration τ_{FWHM}> 7 ns and 1 Hz repetition rate. The pulses were focused on the plate target through an MgF_2 cylindrical lens with the focal length of 30 cm. The incident angle to the target was 45°. The laser spot was set within 3 mm^2. Maximum energy output of 110 mJ/pulse was corresponding to a fluence of ~3.6 J/cm^2. The deposition was made in a stainlees steel vacuum chamber, evacuated to 2×10^{-6} Torr. The target was rotated with the frequency of 0.4 Hz during PLD deposition.

In the next step a $SnSe_2$ layer has been deposited. The obtained double film structure has been repeated two more times, obtaining in total six layers on the substrate as

$Te/SnSe_2/Te/SnSe_2/Te/SnSe_2$. The number of laser pulses for every deposited layer was 30 000. The structure of the triple sandwich deposition has been investigated by X-ray diffraction. A TUR-M62 diffractometer provided with copper target tube has been used.

The gas sensing measurements have been performed in a Gas Mixing Station. The test atmosphere (synthetic air, methane and carbon oxide) of purity 5.0 has been purged at a constant debit (100 ml/min) with a digital Alltech debitmeter. For humidity concentration a barbotting device with distilled water was used.

3. Results

3.1. X-ray diffraction

The $(TeSnSe_2)_3$ multilayer film supported on the body of the sensor device has been investigated by X-ray diffraction. The X-ray pattern of the material just after deposition is shown in Fig. 1. Some intense peaks can be ascribed to Al_2O_3 substrate and to the Pt inter-digitized electrodes. The remaining peaks are attributed to hexagonal tellurium, and to tetragonal TeO_2. The tellurium oxide is due to the reaction of oxygen from the deposition chamber and/or the surface oxidation of the multilayer after several days of maintaining in ambient atmosphere.

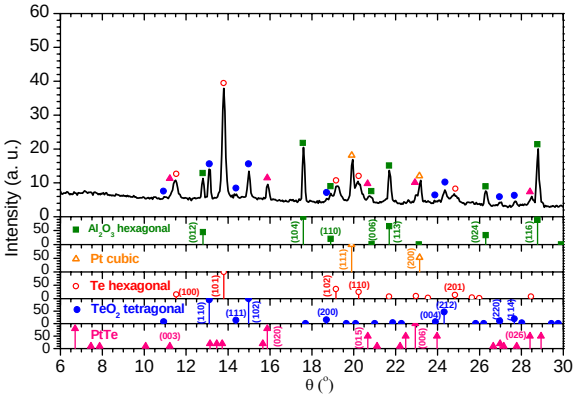

Fig. 1. The X-ray diffraction pattern of the $(Te/SnSe_2)_3$ multilayer film freshly deposited.

After gas sensing investigation the multilayer film was annealed at 500 °C for 6 h in oxygen fluence. The X-ray diagram of the heat treated sample is presented in Figure 2. While the tellurium phase is still preserved, new phases are formed. One phase is the tetragonal $SnSe_2$ phase with a strong orientation along the (001) crystallographic plane, as evidenced by the strong peak situated at ~ 7.2 ° theta. Other minor phase is the SnO_2 tetragonal phase. The amount of TeO_2 phase remains the same.

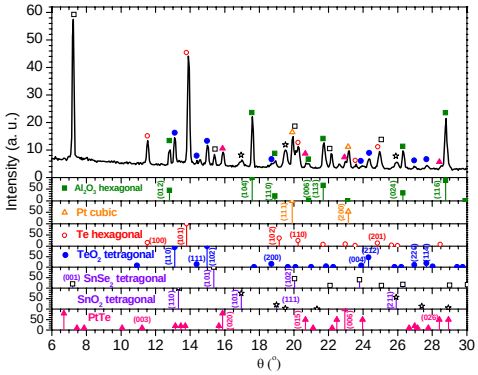

Fig. 2. The X-ray diffraction pattern of the $(Te/SnSe_2)_3$ multilayer film after annealing at 500 °C for 6 hours in oxygen fluence.

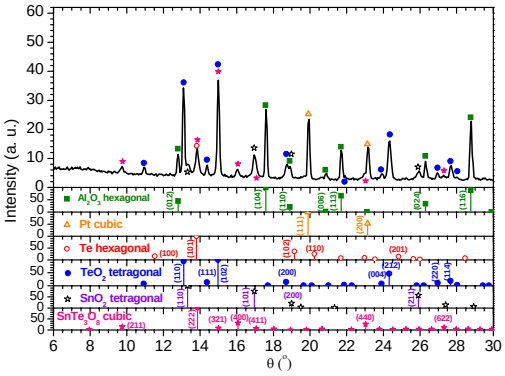

Fig. 3. The X-ray diffraction pattern of the $(Te/SnSe_2)_3$ multilayer film after annealing at 600 °C for 6 hours in oxygen fluence.

After gas sensing investigation the multilayer film was annealed at 600 °C for 6 hours in oxygen fluence. The X-ray diagram of the heat treated sample is presented in Fig. 3. The tellurium phase decreases significantly, while the amount of TeO_2 phase increases.

For SnO_2 some of the peaks are increasing, like those of (110), (101) and (200); the peak (111) vanishes, and (211) remains the same.

A new mixed phase $SnTe_3O_8$ is also revealed on the X-ray diagram.

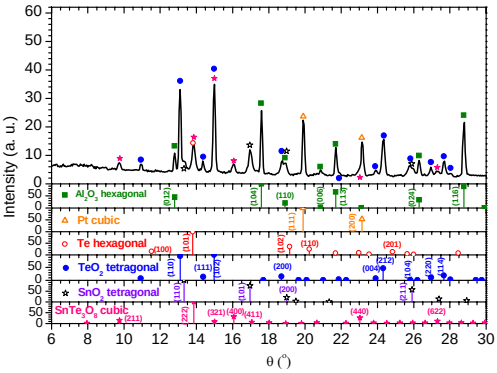

Fig. 4 The X-ray diffraction pattern of the $(Te/SnSe_2)_3$ multilayer film after annealing at 620 °C for 2 hours in oxygen fluence.

After annealing at 620 °C for 2 h in oxygen fluence only (104) TeO_2 peak increases.

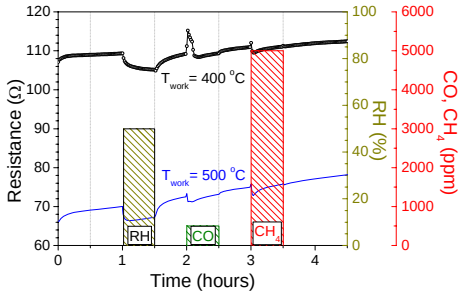

Fig. 5. The behaviour of the multilayer $(Te/SnSe_2)_3$ sensor annealed at 500 °C and measured at working temperatures (T_{work}) of 400 and 500 °C.

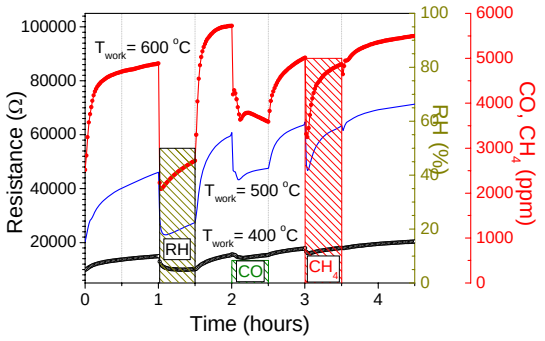

Fig. 6. The behaviour of the multilayer $(Te/SnSe_2)_3$ sensor annealed at 600 °C and measured at working temperatures (T_{work}) of 400, 500 and 600 °C.

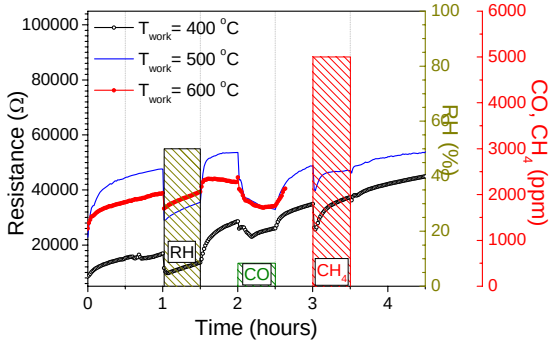

Fig. 7. The behaviour of the multilayer $(Te/SnSe_2)_3$ sensor annealed at 620 °C and measured at working temperatures (T_{work}) of 400, 500 and 600 °C.

The multilayer sensor $(Te/SnSe_2)_3$ has been tested for sensitivity to various gases and humidity at different temperatures of the material.

Fig. 5 shows the sensitivity of the sensor to humidity, carbon oxide and methane at standard thresholds: RH = 50 %; CO = 500 pm; CH_4 = 5000 ppm for annealing temperature of 500 °C. The measurements were carried out at work temperatures of 400 °C and 500 °C.

The sensitivity to gases for the work temperature is low, the maximum sensitivity being for relative humidity (RH) of 50 %. A particular feature regarding the humidity sensing is the gradually decrease of the resistivity when water vapour atmosphere is introduced in the test chamber. Practically, the sensor is not sensible to CO and CH_4. For 500 °C working temperature the sensor exhibits a significant sensing to RH, of the same order of magnitude as in the case of operation at 400 °C, but the trend of the resistivity is to drop to the lowest value immediately after introducing the water vapours. The value is then maintained at a constant value up to the switching off of the humidity inlet. This characteristic may be due to the rapid equilibration of the water at the surface of the sensors for high temperature operation.

The sensor was heat treated at 600 °C. The gas testing results are shown in Fig. 6. For this large annealing temperature (600 °C) the sensitivity of the sensor increases tremendously. The sensitivity at 400 °C is almost similar to the case discussed above. The sensitivity at 500 °C strongly increases if compared to the sensitivity of the sensor annealed at 500 °C. This feature can be related to the special structure of the sensor treated at 600 °C: the amplification of the phases SnO_2 and $SnTe_3O_8$. In the same time the sensitivity to CO increases. The sensitivity to methane is very low. For the highest operation temperature, 600 °C a strong sensitivity to CO is noticed and a significant sensitivity to CH_4 does also appear. For the sensor treated at 620 °C (Fig. 7) the highest sensitivity is against CO even at 500 °C working temperature. No significant sensitivity to methane was revealed. This specific effect can be related to the development of the phase TeO_2.

In Tables 1 and 2 are shown the values of the sensitivity of the sensor (measured by the ratio R_{out}/R_{in}) for different cases of operation temperatures after annealing the sensor material at 500 °C and 600 °C.

Table 1 The sensitivity of the sensor for different gases for the annealing temperature of 500 °C.

Temp	RH	CO	CH4
400	1.03	1.01	1.01
500	1.04	1.01	1.01

Table 2 The sensitivity of the sensor for different gases for the annealing temperature of 600 °C.

Temp	RH	CO	CH4
400	1.48	1.03	1.01
500	1.82	1.29	1.04
600	1.81	1.49	1.06

It seems that the multilayer annealed films are highly sensible to humidity, but also they can operate successfully at 600 °C, in carbon oxide atmosphere.

4. Conclusions

The chalcogenide sensor based on multilayers of composition $(Te/SnSe_2)_3$ deposited by pulsed laser deposition develops during high temperature annealing in oxygen atmosphere several oxide phases: SnO_2, TeO_2 and $SnTe_3O_8$. The $SnTe_3O_8$ phase could be responsible for the response of the sensor to various gases. The sensor annealed at 600 °C is very efficient for the detection of carbon monoxide (CO) and water vapour concentration in atmosphere. The sensor is practically insensible to the methane atmosphere. For annealing at 620 ^oC the sensitivity to CO increases due, probably, to the enhancement of the TeO_2 phase. For annealing temperature at 500 °C the sensor is mostly sensible to the water vapour. A couple of two sensors, one annealed at 500 °C and other at 600 °C can be used for accurate detection of water vapours and of carbon dioxide in the ambient atmosphere, simultaneously.

Acknowledgement

The authors gratefully acknowledge the financing of this work by the Ministry of Education, Research and Youth of Romania through the Matnantech – CeEx Program, Project No. C4/2005.

References

[1] C. Xu, J. Tamaki, N. Miura, N. Yamazoe, Sensors and Actuators **B3**, 147 (1991).
[2] G. Zhang, M. Liu, Sensors and Actuators **B 69**, 144 (2000).
[3] S. G. Ansari, P. Boroojerdian, S. R. Sainkar, R. N. Karekar, R. C. Aiyer, S. K. Kulkarni, Thin Solid Films **295**, 271 (1997).
[4] A. Dieguez, A. Vila, A. Cabot, A. Romano-Rodriguez, J. R. Morante, J. Kappler, N. Bârsan, U. Weimar, W. Göpel, Sensors and Actuators **B68**, 94 (2000).
[5] N. Barsan, D. Koziej, U. Weimar, Sensors and Actuators **B 121**, 18 (2007).
[6] M. Girtan, A. Bouteville, M. Rusu, J. Optoelectron. Adv. Mater. **8**(1), 27 (2006)
[7] G. Fang, Z. Liu, C. Liu, K. Yao, Sensors and Actiators **B66**, 46 (2000).
[8] S. Mihaiu, A. Braileanu, M. Ban, J. Madárasz, G. Pokol, J. Optoelectron. Adv. Mater. **8**(2) 572 (2006).
[9] C. Gumus, O. M. Ozkendir, H. Kavak, Y. Ufuktepe, J. Optoelectron. Adv. Mater. **8**(1), 299 (2006).
[10] C. Baban, Y. Toyada, M. Ogita, J. Optoelectron. Adv. Mater. **7**(2), 891 (2005).
[11] M. Stankova, X. Vilanova, J. Calderer, I. Gràcia, C. Cane, X. Coreig, J. Optoelectron. Adv. Mater. **7**(3), 1237 (2005).
[12] S. Marian, D. Tsiulyanu, H.–D. Liess, Sensors and Actuatos **B 78**, 191 (2001).
[13] B. Georgieva, I. Podolesheva, J. Pirov, V. Platikanova, J. Optoelectron. Adv. Mater. **7**(5), 2595 (2005).
[14] K. P. Kornev, I. P. Korneva, J. Optoelectron. Adv. Mater. **7**(5), 2359 (2005).
[15] A. Tomescu, C. Simion, Optoelectron. Adv. Mater. – Rapid Comm., **1**(3), 118 (2007).
[16] C. Cali, G. Taillades, A. Pradel, M. Ribes, Sensors and Actuators **B 76**, 560 (2001).
[17] Yu. G. Vlasov, Yu. G. Murzina, A. V. Legin, Yu. E. Ermolenko, J. Schubert, M. J. Schüroning, H. Lut, Russian Journal of Applied Chemistry **75**(3), 351 (2002).
[18] K. P. Kornev, I. P. Korneva, J. Optoelectron. Adv. Mater. **7**(5), 2359 (2005).
[19] A. K. Vidybida, A. S. Usenko, A. L. Kukla, A. S. Pavluchenko, O. Yu. Posudievsky, V. D. Pokhodenko, J. Optoelectron. Adv. Mater. **7**(6), 2815 (2005).
[20] A. Tomescu, R. Roescu, J. Optoelectron. Adv. Mater. **7**(3), 1529 (2005).
[21] F. Sava, A. Lörinczi, M. Popescu, G. Socol, E. Axente, I. N. Mihailescu, M. Nistor, J. Optoelectron. Adv. Mater. **8**(4), 1367 (2006).
[22] D. Nesheva, Z. Aneva, S. Reynolds, C. Main, A. G. Fitzgerald, J. Optoelectron. Adv. Mater. **8**(6), 2120 (2006).
[23] D. Luca, J. Optoelectron. Adv. Mater. **7**(2), 625 (2005).
[24] O. F. Caltun, J. Optoelectron. Adv. Mater. **7**(2), 739 (2005).
[25] P. Nemec, J. Jedelsky, M. Frumar, M. Vlcek, J. Optoelectron. Adv. Mater. **7**(5), 2635 (2005).
[26] I. Stanca, J. Optoelectron. Adv. Mater. **8**(3), 1148 (2006).
[27] C. Grigoriu, Y. Kuroki, I. Nicolae, X. Zhu, M. Hirai, H. Suematsu, M. Takata, K. Yatsui, J. Optoelectron. Adv. Mater. **7**(6), 2979 (2005).
[28] A. Og. Dikovska, P. A. Atanasov, C. Vasilev, I. G. Dimitrov, T. R. Stoyanchov, J. Optoelectron. Adv. Mater. **7**(3), 1329 (2005).
[29] D. Miu, J. C. Martinez, H. Adrian, J. Optoelectron. Adv. Mater. **8**(1), 24 (2006).
[30] J. Schubert, M.J. Schöning, C. Schmidt, M. Siegert, St. Mesters, W. Zander, P. Kordos, H. Lüth, A. Legin, Yu.G. Mourzina, B. Seleznev, Yu.G. Vlasov, Applied Physics A: Materials Science & Processing, Vol. 69, Suppl. 1, S 803, 1999.
[31] M. Popescu, A. Lőrinczi, F. Sava, A. Tomescu, C. Simion, I. N. Mihailescu, G. Socol, E. Axente S. Miclos, D. Savastru, Patent deposed, OSIM, No. A / 00941-05.12.2006.

*Corresponding author: lorinczi@infim.ro